ACS Catalysis

Research Article

pubs.acs.org/acscatalysis

Concurrent Hydrogenation of Aromatic and Nitro Groups over Carbon-Supported Ruthenium Catalysts

Patrick Tomkins,[†] Ewa Gebauer-Henke,[†] Walter Leitner,[‡] and Thomas E. Müller*[,†]

[†]CAT Catalytic Center, RWTH Aachen University, Worringerweg 2, 52074 Aachen, Germany

[‡]Institut für Technische und Makromolekulare Chemie, RWTH Aachen University, Worringerweg 1, 52074 Aachen, Germany

Supporting Information

ABSTRACT: The concurrent hydrogenation of aromatic and nitro groups poses particular challenges due to the highly differing adsorption strengths of the two chemical moieties on the surfaces of metal catalysts. In a study of the hydrogenation of nitrobenzene as a model reaction, catalysts of ruthenium supported on carbon nanotubes (Ru/CNT) provided an ideal compromise, allowing for hydrogenation of both the aromatic ring and the nitro group. The use of methyl-labeled substrates enabled tracking the pathway of specific substrates and obtaining insight into the relative rates for the hydrogenation of nitrobenzene and intermediates. Together with findings on the coadsorption of nitrobenzene and aniline on the Ru/CNT catalyst, an advanced mechanistic model for the hydrogenation of nitrobenzene emerges.

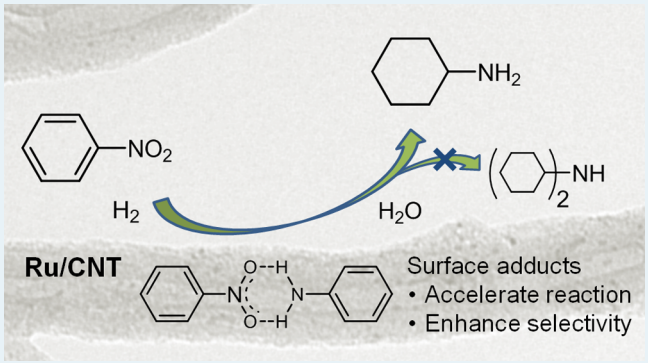

KEYWORDS: *nitrobenzene hydrogenation, amine synthesis, heterogeneous catalysis, reaction network, competitive adsorption, Ru/CNT catalyst*

INTRODUCTION

Many important fine chemicals,[1] agrochemicals,[2,3] pharmaceuticals,[4] and polymer building blocks have been characterized by the presence of multiple functional groups. Selective hydrogenation of corresponding precursor molecules bearing several unsaturated moieties is frequently applied to generate these functional groups.[5−10] However, with heterogeneous catalysts, the presence of a strongly coordinating functional group poses particular challenges for the hydrogenation of more weakly adsorbing groups. Further complexity arises when starting materials and intermediates compete with each other for adsorption on the metal surface.

An industrially relevant example is the hydrogenation of nitroaromatic compounds to the corresponding cycloaliphatic primary amines.[11−13] In such nitroaromatic compounds, the aromatic ring is electron deficient due to the strong electron-withdrawing effect of the nitro group.[14] Consequently, the aromatic ring coordinates only weakly to metals typically employed in hydrogenation reactions.[15] In contrast, the nitro group is strongly coordinating.[16] Due to the competing adsorption modes,[17] the nitro group has a high propensity to being hydrogenated first (Scheme 1, path A/B). However, the aromatic moiety can also be hydrogenated first (path C/D), as reported for substrates where the aromatic ring and nitro group are not directly linked.[18] Also conceivable is a direct hydrogenation pathway that does not involve desorption of an intermediate from the catalyst surface. When a Langmuir−Hinshelwood-type mechanism applies, the prevailing pathway is ruled by the propensity of the particular group to be chemisorbed on the metal surface.[7,19−23]

Scheme 1. Analysis of Possible Reaction Pathways for the Hydrogenation of Nitrobenzene and Methyl-Substituted Analogues

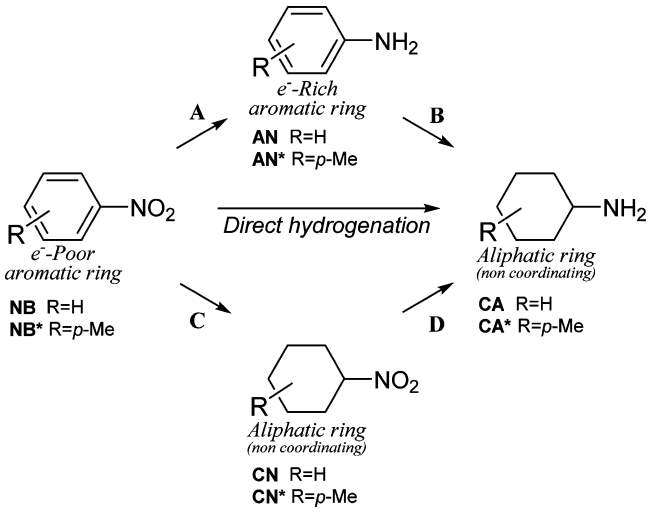

Received: August 2, 2014
Revised: November 9, 2014
Published: November 18, 2014

The aromatic amino intermediate (here aniline) formed during path A/B is very different in character in comparison to the original nitroaromatic compound. The aromatic ring is electron rich due to the electron-donating mesomeric effect of the amino group.[24] Consequently, the aromatic ring is expected to coordinate more strongly to the metal in comparison to the nitroaromatic compounds. However, also the amino group, bearing a lone electron pair strongly localized on nitrogen, tends to coordinate strongly to metal surfaces. Even more pronounced, the amino group in the fully hydrogenated cyclohexylamine is strongly basic. Consequently, the amino groups compete with the aromatic rings and the nitro groups for adsorption on the coordination sites, giving rise to potential product inhibition.[25]

An ideal catalyst for the hydrogenation of such nitroaromatic compounds ought to be equally active for all moieties to be hydrogenated, while nonproductive adsorption modes should have a low probability of occurring. Accordingly, all moieties to be hydrogenated should adsorb with comparable strength to the catalyst surface. Vice versa, the binding constant for the saturated product(s) should be low to avoid product inhibition.

In the synthesis of primary amines, an additional challenge arises from condensation reactions,[26−29] which cause reduced yields through the formation of secondary and tertiary amines,[30] azobenzene, and other coupling products.[31]

In this study, we have explored the hydrogenation of nitrobenzene as a model system for other nitroaromatic compounds. In an exploratory study on the choice of the metal,[38] ruthenium emerged as an ideal candidate. The relative rates for the hydrogenation of nitrobenzene and intermediates were followed in a cohydrogenation study, whereby the path of individual substrates was traced by labeling certain precursors with a methyl substituent. This enables following the reaction pathways that lead to condensation products and recognizing key factors that control chemoselectivity.

EXPERIMENTAL SECTION

Materials. All chemicals were obtained from commercial suppliers and used as received. The carbon-supported catalysts Ru/C, Rh/C, Pd/C, and Pt/C (5 wt % metal) were obtained from Aldrich. Multiwall carbon nanotubes (CNTs) from a chemical vapor deposition process (BAYTUBES C 150 P, Bayer MaterialScience) were used as support for the Ru/CNT catalyst. The CNTs had an average length in the range of 1−10 μm and a mean outer diameter of 13−16 nm. Irregularly shaped CNTs were aggregated to lose agglomerates with 1−3 mm diameter.

Catalyst Preparation. The Ru/CNT catalyst was prepared by the deposition precipitation method. For this, CNTs (20 g) were suspended in refluxing nitric acid (65%, 150 mL) for 2 h. Subsequently, the CNTs were filtered off, washed with deionized water until the eluent had a neutral pH value, and dried. The treated CNTs (10.045 g) were resuspended in an aqueous solution (300 mL) of urea (1.462 g, 24.3 mmol), $Ru(NO)(NO_3)_x(OH)_y$ (aqueous solution, ∼1.5 wt % Ru), and nitric acid (32.4288 g). The mixture was stirred under Ar at 90 °C for 22 h. The CNTs were filtered off, washed with a small amount of water, and dried under a flow of argon (100 mL/min) at 120 °C for 2 h. Subsequently, the ruthenium precursor was reduced under a flow of hydrogen (100 mL/min) at 200 °C for 1 h.

Catalyst Characterization. Prior to the hydrogenation experiments, the catalysts were characterized in detail. The data are summarized in the Supporting Information.

Hydrogenation Experiments. Hydrogenation reactions were carried out in a 200 mL stainless steel autoclave equipped with gas entrainment stirrer, heating mantel, and sampling valve. The autoclave was charged with substrate, THF, catalyst, and internal standard (dodecane in the case of NB hydrogenation, tetradecane when methyl-substituted substrates were used) (Supporting Information). The mixture was heated to the reaction temperature (140 °C, if not stated otherwise), and the reaction was started by pressurizing the autoclave with hydrogen to 100 bar. Samples of the liquid phase were taken during the reaction for analysis by gas chromatography. Concentrations are given as the molar fraction of the particular substance c_i normalized to the initial concentration of the substrate ($c_i/c_{substrate,t=0} \times 100$ mol %). Rates of reaction (r_i) were calculated at 50% of the maximum concentration of compound i by fitting the time−concentration diagrams with a five-parameter logistic function.[32]

RESULTS AND DISCUSSION

In an exploratory study, the most suitable metal for the hydrogenation of nitrobenzene (NB) was explored (Table 1).

Table 1. Hydrogenation of Nitrobenzene with Carbon-Supported Catalysts

catalyst	t_{95}[a] (min)	S_{AN}[b] (%)	S_{CA}[b] (%)	S_{DA}[b] (%)	S_{PC}[b] (%)
Ru/C	24	1.6	90.2	8.2	0
Rh/C	28	1.2	85.3	13.6	0
Pd/C	19	36.5	15.1	17.7	1.5
Pt/C	21	87.2	11.2	13.6	0.4

[a]Time until 95% conversion of nitrobenzene had been achieved. [b]Selectivity after 180 min, full conversion of NB obtained in all cases. Abbreviations: aniline (AN), cyclohexylamine (CA), dicyclohexylamine (DA), phenylcyclohexylamine (PC).

Carbon was chosen as a chemically quite inert support to skirt condensation reactions known for more acidic oxidic supports.[33−35] The catalysts Ru/C, Rh/C, Pd/C, and Pt/C showed similar activities with respect to the hydrogenation of NB, leading to 95% conversion of NB within 19−28 min. As in related hydrogenation reactions,[36] two different classes of catalysts emerged with respect to the chemoselectivity. Ruthenium and rhodium provided cyclohexylamine (CA) in high selectivity. Only a small amount of the condensation product dicyclohexylamine (DA) was formed. In contrast, palladium and platinum provided aniline (AN) as the main product. Thus, only ruthenium and rhodium fulfilled the stated requirements of a catalyst concerning high propensity for hydrogenation of the aromatic ring.[37,38] Ruthenium showed a higher selectivity to the targeted primary amine, whereas a significantly higher amount of the condensation product DA was formed over rhodium. Therefore, ruthenium was chosen for more detailed studies.

Catalyst Synthesis. Being a well-defined carbon support, carbon nanotubes (CNTs) were chosen.[39] To anchor the ruthenium particles on the surface of the CNT, oxidic groups were generated by treatment in refluxing nitric acid.[40] In the next step, a ruthenium precursor was placed evenly on the surface of the CNT by the deposition−precipitation method,[41] which was followed by reducing the precursor to metallic

dx.doi.org/10.1021/cs501122h | ACS Catal. 2015, 5, 203−209

ruthenium with molecular hydrogen. The Ru/CNT catalyst thus obtained had a ruthenium content of 3.6 wt %. Transmission electron microscopy (TEM) measurements showed that small ruthenium particles with a mean diameter of 1.5 nm and a standard deviation of 0.3 nm were evenly distributed over the outer surface of the carbon nanotubes, giving rise to a BET surface area of 210 m^2 g^{-1} (Figure 1). The

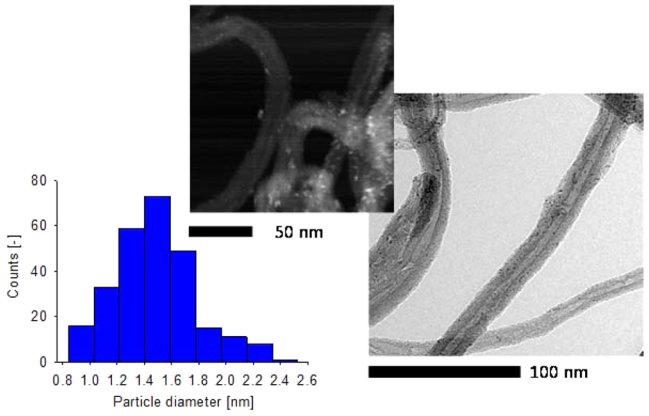

Figure 1. Particle-size distribution of Ru/CNTs used in this study and representative scanning and bright field transmission electron microscopy images (insert and right, respectively).

small diameter of the Ru particles and the absence of larger Ru crystallites were confirmed by H_2 chemisorption and XRD analysis. Macropores formed through aggregation of the irregularly shaped CNT to agglomerates with 1−3 mm diameter enabled rapid intraparticle transport of the reactants.

Reaction Sequence of Nitrobenzene Hydrogenation over Ru/CNT. To obtain insight into the reaction sequence, the hydrogenation of NB over Ru/CNT was followed with time (Figure 2). Immediately after the autoclave was pressurized, the

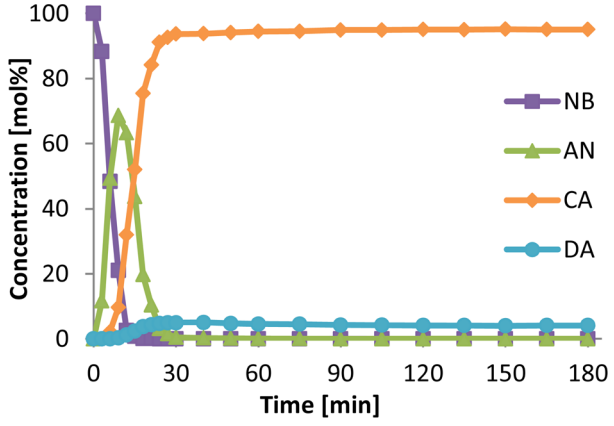

Figure 2. Time−concentration diagram for the hydrogenation of nitrobenzene (NB) over Ru/CNTs (NB/Ru = 160) to intermediately formed aniline (AN) and the final products cyclohexylamine (CA) and dicyclohexylamine (DA).

hydrogenation of NB commenced, and AN was formed as the initial product. Notably, with Ru/CNT full conversion was obtained more rapidly (12 min to >95% conversion) than with Ru/C (27 min). The AN concentration reached a maximum (64 mol %) after 9 min and decreased thereafter. With a time delay of 6 min, CA was formed. After another 3 min, also the formation of DA commenced. Hence, a consecutive reaction according to path A/B (Scheme 1) prevailed. This was verified by plotting the ratios of the concentrations of NB/CA, NB/AN, AN/CA, and AN/DA vs time.[42] In all cases, the ratio extrapolated to zero time increased to infinity (Supporting Information). From this, it was inferred that AN is a consecutive product of NB (Scheme 2, step A) and that CA

Scheme 2. Analysis of Possible Reaction Steps for the Formation of Condensation Products during the Hydrogenation of NB to CA

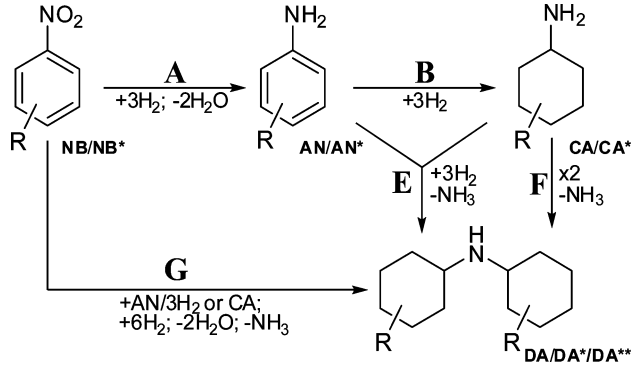

and DA are consecutive products of AN (steps B and E, respectively). The CA/DA ratio decreased rapidly during the reaction to level out at a value of about 20, implying that DA is a consecutive product of CA (step E or F). Closer inspection of the GC chromatograms revealed that traces of nitrosobenzene were formed as intermediates and that a trace amount (<1 mol %) of cyclohexanol was obtained as a side product. Other intermediates and side products mentioned in the literature were not detected under our conditions.[37,43,44]

Cohydrogenation of Nitrobenzene and Aniline. To investigate the relative rates of the hydrogenation of nitro compounds and aromatic amines, an equimolar mixture of NB and AN was hydrogenated (Figure 3). In order to trace the pathway of the different substrate molecules, the nitrobenzene was labeled with a methyl substituent. An initial experiment on the hydrogenation of methylnitrobenzene (NB*) provided a very similar profile and showed only slightly enhanced rates in

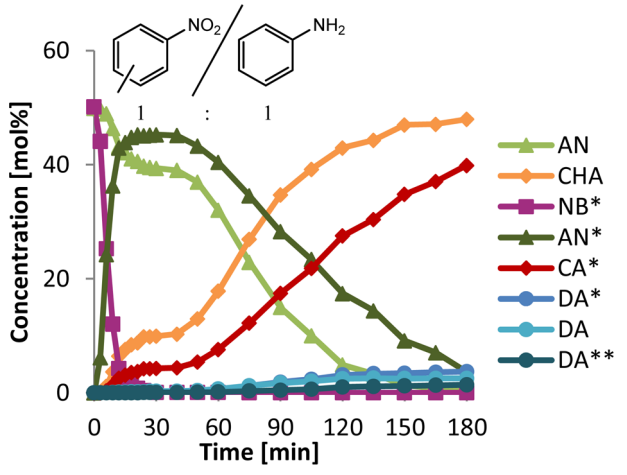

Figure 3. Time−concentration diagram for the cohydrogenation of NB* and an equimolar amount of AN over Ru/CNT (NB*/Ru = 630). The amount of catalyst was adjusted in such a way that comparable reaction times were achieved.

dx.doi.org/10.1021/cs501122h | ACS Catal. 2015, 5, 203−209

comparison to the hydrogenation of NB. This is consistent with the somewhat higher electron density in the aromatic ring of NB* caused by the inductive effect of the methyl group.

During the cohydrogenation of NB* and AN (Figure 3) NB* was converted rapidly (−71.2 mol (mol of Ru)$^{-1}$ min^{-1}, Table 2) to *p*-toluidine (AN*) and was consumed entirely within 30 min. In contrast, AN hydrogenation commenced only after a short lag phase (6 min) with a relatively low rate (−7.3 mol (mol of Ru)$^{-1}$ min^{-1}). Unexpectedly, the consumption of AN slowed down even further after approximately 20 min. The period of slow AN conversion (ca. 20 min) was characterized by a high concentration of AN* of ca. 45 mol %. Thereafter, the consumption of AN as well as of AN* resumed, with the concentration of AN decreasing twice as fast as that of AN* (−7.3 and −4.0 mol (mol of Ru)$^{-1}$ min^{-1}, respectively). The two primary aliphatic amines 4-methylcyclohexylamine (CA*) and CA were obtained as the main products in a ratio of 47/53.

Table 2. Normalized Rates for the Hydrogenation of Nitrobenzene and Corresponding Reference Reactions

	rate (mol (mol of Ru)$^{-1}$ min^{-1})[b]					
reagents[a]	NB	NB*	AN	AN*	CA	CA*
NB/−/−	−20.4		−13.4		13.1	
NB*/−/−		−22.9		−14.6		13.1
NB*/AN/−[c]		−71.2	−7.3	−4.0	7.3	4.0
NB*/AN/−[d]		−3.3	−35.6	−1.0	34.2	0.8
NB*/−/CA		−72.4		−2.8		2.9
−/AN*/CA				−15.0		13.6
−/AN/−			−13.5		13.0	

[a]Substrates labeled with a methyl substituent are marked with an asterisk. [b]Rates at 50% of the maximum concentration of the corresponding compound. [c]Initial ratio NB*/AN 1/1. [d]Initial ratio NB*/AN 1/19.

Inspection of the concentration profiles of secondary amine formation shows that there was only a small amount of secondary amines formed as long as NB* was present (<50 min). Thereafter DA and DA* were formed until the corresponding aniline was depleted, indicating that the aromatic amine plays a key role in the formation of secondary amines (step E).

Surprisingly, the rate of NB* conversion was about 3 times higher, on cohydrogenation in the presence of AN, on comparison to the hydrogenation of NB* as the sole substrate. This goes along with an enhanced rate of formation of CA and CA* during the first 30 min. Once NB* had been consumed, also the formation of CA* from AN* slowed down, thereby indicating that the surface coverage with substrate molecules changes at this stage of the reaction. Once a new steady state had been established on the catalyst surface, the reaction rate increased again. These findings clearly show that the rate of nitroarene hydrogenation can be increased by the addition of aromatic amine to the initial reaction mixture. Vice versa, the rate of aniline hydrogenation is also influenced, albeit to a smaller extent.

To corroborate that the presence of nitro compounds leads to an increase in the rate of aniline hydrogenation, NB* and AN were also cohydrogenated in a molar ratio of 1/19 (Figure 4). After an initiation period of 6 min, AN was hydrogenated to CA. The rate of AN consumption (−35.6 mol (mol of Ru)$^{-1}$ min^{-1}) was enhanced significantly in comparison to the hydrogenation of AN as the sole substrate (−13.5 mol (mol of Ru)$^{-1}$ min^{-1}, Table 2). Once the last traces of nitro compound had been consumed (after 30 min), the rate of AN hydrogenation slowed down. Clearly, the presence of a nitro compound had a promoting effect on aniline hydrogenation.

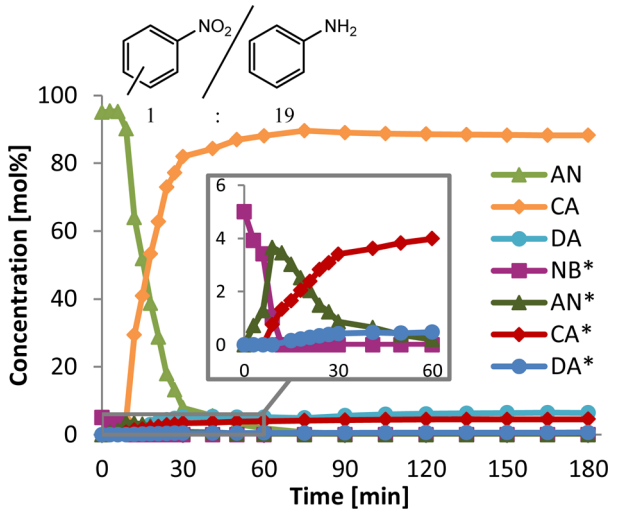

Figure 4. Time−concentration diagram for the cohydrogenation of NB* and AN (molar ratio 1/19) over Ru/CNT (AN/Ru = 630). The inset shows an enlarged representation of the profiles for the labeled compounds.

Pathways to the Formation of Secondary Amines. Insight into the role of NB in the formation of secondary amines was obtained by the hydrogenation of NB* in the presence of an equimolar amount of CA (Figure 5). NB* was converted at a high rate (−72.4 mol of NB* (mol of Ru)$^{-1}$ min^{-1}, step A) to AN*. In a slow consecutive reaction, AN* was hydrogenated to CA* (−2.8 mol of AN* (mol of Ru)$^{-1}$ min^{-1}, step B), while the concentration of CA remained nearly constant. Thus, the direct condensation of primary to secondary amines is of minor importance (step F). While NB* was hydrogenated (<20 min), there was hardly any formation of secondary amines, showing that the nitroaromatic compound did not participate in the formation of secondary amines (step G). At longer reaction times, DA* and DA**

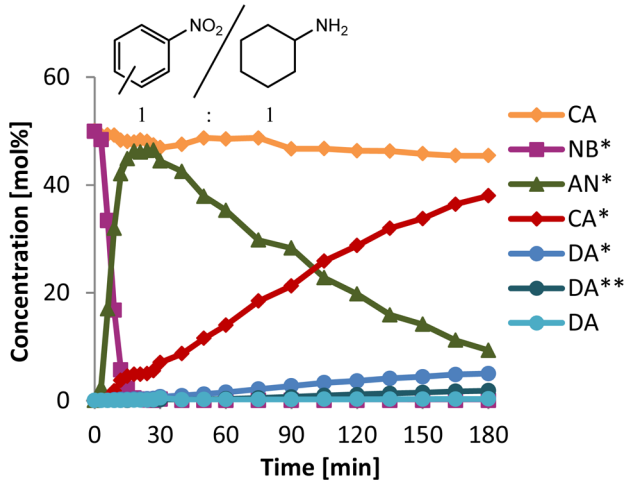

Figure 5. Time−concentration diagram for the hydrogenation of NB* in the presence of an equimolar amount of CA over Ru/CNT (NB*/Ru = 630).

dx.doi.org/10.1021/cs501122h | ACS Catal. 2015, 5, 203−209

were formed in parallel once an increasing concentration of CA* became available in the reaction mixture (Supporting Information). Thus, DA*, DA**, and CA* are consecutive products of AN*, but formation of DA* and DA** also requires the presence of CA and/or CA* (step E). In addition, the absence of aromatic secondary amines suggests that secondary amines are formed from partially hydrogenated AN derivatives and/or fully hydrogenated amines.

The role played by the aromatic and aliphatic amines in the formation of secondary amines (steps E and F) was thus explored in the next step. For this, AN* was hydrogenated in the presence of an equimolar amount of CA (Figure 6). After a

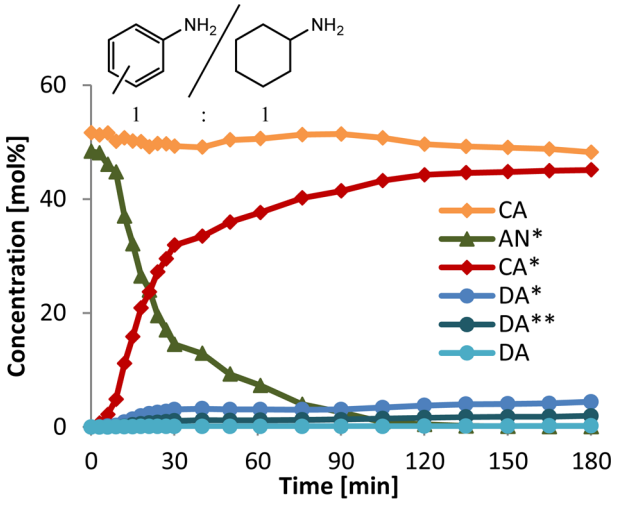

Figure 6. Hydrogenation of AN* in the presence of an equimolar amount of CA over Ru/CNT (AN*/Ru = 630).

short lag phase, the concentration of AN* decreased exponentially. In parallel, CA* was formed as the main product. In contrast, the concentration of CA remained nearly constant. Closer inspection of the profile of formation of secondary amines revealed that the concentration of DA* and DA** increased during the initial phase of the reaction. After 30 min the concentration of the two secondary amines leveled off at 3 and 1 mol %, respectively. The concentration of DA remained insignificant over the entire time range.

In the initial phase of the reaction, DA* and DA** were formed in a ratio exceeding 4/1, which decreased to approximately 2/1 at longer reaction times. This confirms that most of the secondary amine is formed by reaction of AN* with the aliphatic amine (CA or CA*) present in the reaction mixture (step E). One possibility is the reaction of adsorbed AN* or of a consecutive partially hydrogenated surface intermediate[37] with coadsorbed aliphatic amine. In contrast, a prevailing pathway via condensation of two surface intermediates resulting from AN* would result in the exclusive formation of DA**. The low amount of DA formed corroborates that also the direct condensation of CA was insignificant (step F). Only at higher temperatures (180 °C) did the condensation of CA to DA become significant once AN had been converted fully. Moreover, condensation products with one aromatic and one aliphatic ring were not detected, indicating that the direct condensation of aniline and primary amines is insignificant.

Kinetic and Mechanistic Model. The key findings of the preceding experiments allow elucidation of the reaction pathways to formation of cyclohexylamine and secondary amines, as follows.

(I) The hydrogenation of NB to CA proceeds via AN as intermediate (path A/B), while the pathway via nitrocyclohexane (path C/D) and direct hydrogenation are insignificant (Scheme 1).

(II) In the presence of an aromatic amine (AN) at the initial stage of the reaction, NB is hydrogenated at a considerably higher rate.

(III) NB is hydrogenated quite selectively to AN (step A) and does not contribute to the formation of DA (Scheme 2, step G).

(IV) The predominant condensation reaction comprises AN as well as CA (step E). Most likely, a partially hydrogenated AN derivative reacts on the ruthenium surface with CA.

(V) Although feasible, the condensation of two CA molecules occurs at a relatively low rate (step F).

The reaction pathway NB → AN → CA (key finding I) is consistent with a strong preference of nitrobenzene to coordinate via the nitro group and not via the electron-deficient aromatic ring. In contrast, aniline has a sufficiently high propensity to coordinate via the (relatively electron rich) aromatic ring, which allows the ring to be hydrogenated.

To explain the enhanced reaction rate (key finding II), we propose that NB and AN coadsorb on the surface of the catalyst, forming a hydrogen-bonded adduct (Scheme 3). Such

Scheme 3. Adduct Proposed To Be Formed during the Hydrogenation of Nitrobenzene and Stabilization of the Intermediate Enamine against Nucleophilic Attack of an Amine on an Imine Intermediate

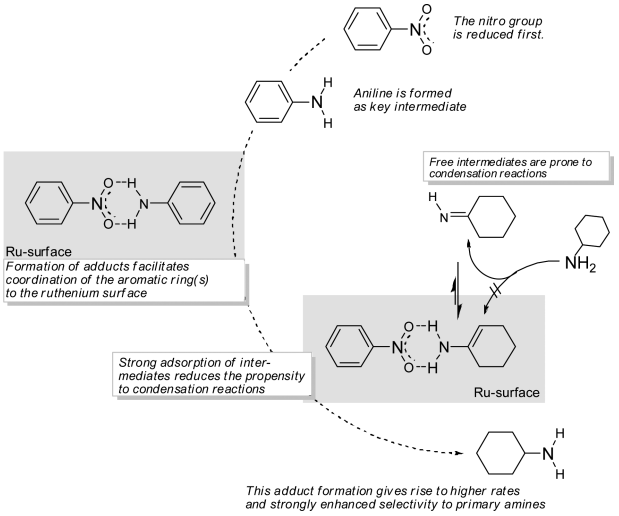

adduct formation is well-known for organic nitro compounds and aromatic amines (Supporting Information).[45−52] The adduct formation between NB and AN allows for faster hydrogenation of the nitro group. The presence of an aliphatic amine (CA) has a similar effect. Vice versa, when AN is hydrogenated in the presence of a small amount of nitroaromatics, the rate of AN hydrogenation is enhanced. Also in this case, we propose that NB and AN form a hydrogen-bonded adduct on the surface of the catalyst. In this context, we found recently that the addition of $NaNO_2$ in the hydrogenation of toluidines results in an increased rate,[53] most likely due to formation of an adduct of nitrite and aromatic amine on the catalyst surface.[11,54]

dx.doi.org/10.1021/cs501122h | ACS Catal. 2015, 5, 203−209

The main condensation reaction (key findings III–V) most likely involves reduction of AN to the enamine. The latter tautomerizes to the corresponding imine, which is susceptible to nucleophilic attack by CA. Nitrobenzene stabilizes the enamine by formation of a hydrogen-bonded aggregate on the catalyst surface (Scheme 3), thereby reducing the probability that the condensation reaction occurs.

Adsorption Measurements. To clarify the interaction, the competitive adsorption of NB and AN on the catalyst surface was explored on the basis of the frontal analysis method.[55] For this, a chromatographic column was filled with Ru/CNT and the breakthrough of a mixture of NB and AN was followed (Figure 7). The breakthrough of NB commenced shortly (at 12

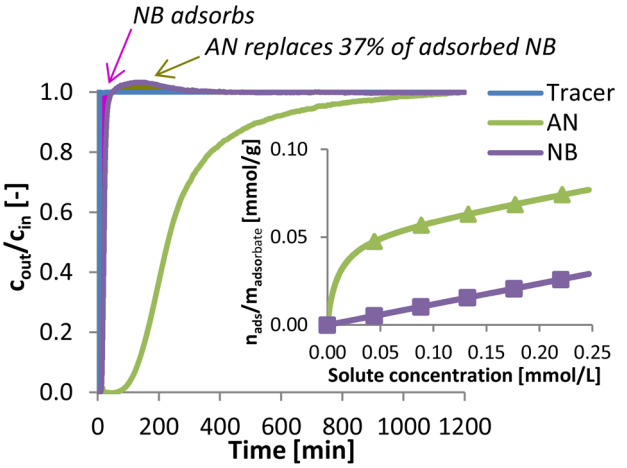

Figure 7. Breakthrough curve for competitive adsorption of AN and NB in comparison to that of a nonadsorbing tracer (1,3,5-tri-*tert*-butylbenzene) and isotherms for the respective adsorption of AN and NB on Ru/CNT (inset, 0.31 mmol of Ru (g of cat)$^{-1}$).

min) after the breakthrough of a nonadsorbing tracer (1,3,5-tri-*tert*-butyl-benzene, at 5 min). Quantification of the breakthrough curve revealed that one NB molecule was adsorbed for every 8.6 Ru atoms in the Ru/CNT catalyst. Interestingly, the concentration of NB then went through a maximum (at 134 min) to decrease thereafter to the steady-state concentration. Such a maximum in the NB concentration clearly demonstrates that NB and AN adsorb on the same sites. Quantification showed that AN from the feed displaced 37% of the already adsorbed NB (rollover effect).[55] Thus, roughly equimolar amounts of NB and AN are coadsorbed on the catalyst surface fully consistent with the formation of hydrogen-bonded adducts, giving rise to an ideal coverage on the catalyst's surface for the hydrogenation reaction to proceed.

Similarly, the adsorption isotherms determined by the single-solute breakthrough measurements (Figure 7, insert) were characterized by a linear term with approximately equal slope. Most likely, this linear term of the isotherms corresponds to adsorption on metallic ruthenium. Here, both NB and AN adsorb on the same sites with similar adsorption constants. As the breakthrough of AN commenced much later than that of NB (75 min) and the adsorption isotherm was characterized by a rapid increase at low solute concentrations, a large amount of AN must bind to a second type of adsorption sites. While both NB and AN may interact weakly with the surface of the CNT support,[56] only the more basic AN readily binds to Brønsted acid sites generated in the initial acid pretreatment of the CNT.

CONCLUSIONS

The hydrogenation of nitrobenzene over Ru/CNT was studied as a model reaction for the concurrent catalytic reduction of an aromatic ring in the presence of a strongly coordinating nitro group. Our exploratory experiments showed that Ru/CNT is an ideal choice, combining high activity with excellent chemoselectivity to the targeted primary amine. Ruthenium distinguishes itself by comparable rates for the hydrogenation of the aromatic ring and of the nitro group.

Interestingly, the presence of aniline at the initial phase of the reaction considerably promoted the rate of nitrobenzene hydrogenation. Similarly, in the presence of small amounts of nitrobenzene, aniline was hydrogenated at an increased rate. We propose that nitrobenzene and aniline form a hydrogen-bonded aggregate, which binds to the ruthenium surface in such a way that the aromatic ring is enabled to coordinate to the surface.

Hardly any condensation reactions took place as long as nitrobenzene was present in the reaction mixture. This results in a strongly enhanced selectivity to primary amines. Condensation products form only at a later stage of the reaction. Tracking the pathway of specific substrates revealed that the prevailing condensation pathway involves the reaction of partially hydrogenated aniline derivatives with cyclohexylamine on the surface of the ruthenium catalyst.

Such concurrent hydrogenation of multiple functional groups in selected precursor molecules provides ready access to multifunctional molecules. A detailed knowledge of the relative reaction rates in the resulting complex reaction networks is the basis for the rational design of the corresponding synthetic strategies.

ASSOCIATED CONTENT

Supporting Information

The following file is available free of charge on the ACS Publications website at DOI: 10.1021/cs501122h.

Experimental details, catalyst characterization, complementary kinetic data, and data on adduct formation (PDF)

AUTHOR INFORMATION

Corresponding Author

*T.E.M.: e-mail, thomas.mueller@catalyticcenter.rwth-aachen.de; fax, +492418022593; tel, +492418028594.

Notes

The authors declare no competing financial interest.

ACKNOWLEDGMENTS

We thank Cleopatra Herwartz (GfE) for taking the TEM images, Xaver Hecht (TUM) for the BET measurements, Elise Keitel (IME) for the elemental analyses, Julia Wurlitzer (ITMC) for developing the GC method, Gergana Ivanova for catalyst tests, and Daniel Hönders for implementing the frontal analysis method at CAT Catalytic Center. The staff of the mechanical workshop at ITMC is acknowledged for their support.

REFERENCES

(1) Sheldon, R. A.; van Bekkum, H. *Fine Chemicals through Heterogeneous Catalysis*; Wiley: Hoboken, NJ, 2008.

(2) Godfrey, C. R. A. *Agrochemicals from Natural Products*; Marcel Dekker: New York, 1995.

(3) Plimmer, J. R.; Gammon, D. W.; Ragsdale, N. N. *Encyclopedia of Agrochemicals*; Wiley: Hoboken, NJ, 2003; Vols. *1*−*3*.
(4) Cutler, S. J.; Cutler, H. G. *Biologically Active Natural Products: Pharmaceuticals*; Taylor & Francis: London, 2000.
(5) Makosch, M.; Lin, W.-I.; Bumbálek, V.; Sá, J.; Medlin, J. W.; Hungerbühler, K.; van Bokhoven, J. A. *ACS Catal.* **2012**, *2*, 2079−2081.
(6) Hitzler, M. G.; Smail, F. R.; Ross, S. K.; Poliakoff, M. *Org. Process Res. Dev.* **1998**, *2*, 137−146.
(7) Boronat, M.; Corma, A. *Langmuir* **2010**, *26*, 16607−16614.
(8) Cárdenas-Lizana, F.; Berguerand, C.; Yuranov, I.; Kiwi-Minsker, L. *J. Catal.* **2013**, *301*, 103−111.
(9) Joannet, E.; Horny, C.; Kiwi-Minsker, L.; Renken, A. *Chem. Eng. Sci.* **2002**, *57*, 3453−3460.
(10) Nishimura, S. *Handbook of heterogeneous catalytic hydrogenation for organic synthesis*; Wiley: Hoboken, NJ, 2001.
(11) Oh, S. G.; Mishra, V.; Cho, J. K.; Kim, B.-J.; Kim, H. S.; Suh, Y.-W.; Lee, H.; Park, H. S.; Kim, Y. J. *Catal. Commun.* **2014**, *43*, 79−83.
(12) Weissermel, K.; Arpe, H. J. *Industrial Organic Chemistry*; Wiley-VCH: Weinheim, Germany, 2003.
(13) Kraynov, A.; Gebauer-Henke, E.; Leitner, W.; Müller, T. E. *Al'tern. Energ. Ekol.* **2010**, *4*, 37−44 ISSN 1608-8298.
(14) Lipkowitz, K. B.; Chang, C. P. *J. Am. Chem. Soc.* **1982**, *104*, 2647−2648.
(15) Bond, G. C.; Keane, M. A.; Kral, H.; Lercher, J. A. *Catal. Rev. Sci. Eng.* **2000**, *42*, 323−384.
(16) Boronat, M.; Concepción, P.; Corma, A.; González, S.; Illas, F.; Serna, P. *J. Am. Chem. Soc.* **2007**, *129*, 16230−16237.
(17) Kahl, T.; Schröder, K.-W.; Lawrence, F. R.; Marshall, W. J.; Höke, H.; Jäckh, R. In *Ullmann's Encyclopedia of Industrial Chemistry*; Wiley-VCH: Weinheim, Germany, 2000.
(18) Young, D. V.; Snyder, H. R. *J. Am. Chem. Soc.* **1961**, *83*, 3160−3161.
(19) Delbecq, F.; Loffreda, D.; Sautet, P. *J. Phys. Chem. Lett.* **2010**, *1*, 323−326.
(20) Somorjaia, G. A. *Appl. Surf. Sci.* **1997**, *121*−*122*, 1−19.
(21) Zaera, F. *Phys. Chem. Chem. Phys.* **2013**, *15*, 11988−12003.
(22) Sachtler, W. M. H.; Van Der Plank, P. *Surf. Sci.* **1969**, *18*, 62−79.
(23) Somorjai, G. A.; Rupprechter, G. *Stud. Surf. Sci. Catal.* **1997**, *109*, 35−59.
(24) Schaefer, T.; Schneider, W. G. *Can. J. Chem.* **1963**, *41*, 966−982.
(25) Briggs, J. P.; Yamdagni, R.; Kebarle, P. *J. Am. Chem. Soc.* **1972**, *94*, 5128−5130.
(26) Gomez, S.; Peters, J. A.; Maschmeyer, T. *Adv. Synt. Catal.* **2002**, *344*, 1037−1057.
(27) Schärringer, P.; Müller, T. E.; Jentys, A.; Lercher, J. A. *J. Catal.* **2009**, *263*, 34−41.
(28) Schärringer, P.; Müller, T. E.; Lercher, J. A. *J. Catal.* **2008**, *253*, 167−169.
(29) Chojecki, A.; Veprek-Heijman, M.; Müller, T. E.; Schärringer, P.; Veprek, S.; Lercher, J. A. *J. Catal.* **2006**, *245*, 237−248.
(30) Winans, C. F.; Adkins, H. *J. Am. Chem. Soc.* **1932**, *54*, 306−312.
(31) Gelder, E. A.; Jackson, S. D.; Lok, C. M. *Chem. Commun.* **2005**, *4*, 522−524.
(32) Gottschalk, P. G.; Dunn, J. R. *Anal. Biochem.* **2005**, *343*, 54−65.
(33) Campbell, C. T.; Grant, A. W.; Starr, D. E.; Parker, S. C.; Bondzie, V. A. *Top. Catal.* **2001**, *14*, 43−51.
(34) Campbell, C. T. *Acc. Chem. Res.* **2013**, *46*, 1712−1719.
(35) de Jongh, P. *Catalysis* **2012**, *144*, 431−432.
(36) Gebauer-Henke, E.; Leitner, W.; Prokofieva, A.; Vogt, H.; Müller, T. E. *Catal. Sci. Techn.* **2012**, *2*, 2539−2548.
(37) Greenfield, H. *J. Org. Chem.* **1964**, *29*, 3082−3084.
(38) Rylander, P. N.; Steele, D. R. *Engelhard Industries Technical Bulletin*; Engelhard Industries: Newark, NJ, 1962; Vol. 3, pp 19−22.
(39) Schaetz, A.; Zeltner, M.; Stark, W. J. *ACS Catal.* **2012**, *2*, 1267−1284.
(40) Datsyuk, V.; Kalyva, M.; Papagelis, K.; Parthenios, J.; Tasis, D.; Siokou, A.; Kallitsis, I.; Galiotis, C. *Carbon* **2008**, *46*, 833−840.
(41) Chorkendorff, I.; Niemantsverdriet, J. W. *Concepts of Modern Catalysis and Kinetics*; Wiley: Hoboken, NJ, 2007.
(42) Zhao, Y.; Kukula, P.; Prins, R. *J. Catal.* **2004**, *221*, 441−454.
(43) Stork, G.; White, W. N. *J. Am. Chem. Soc.* **1956**, *78*, 4604−4619.
(44) Winans, C. F. *Ind. Eng. Chem.* **1940**, *32*, 1215−1216.
(45) Steiner, T. *Angew. Chem., Int. Ed.* **2002**, *41*, 48−76.
(46) Landenberger, K. B.; Matzger, A. J. *Cryst. Growth Des.* **2010**, *10*, 5341−5347.
(47) Smith, G.; Wermuth, U. D.; Young, D. J.; White, J. M. *Acta Crystallogr.* **2009**, *C65*, o543−o548.
(48) Fallon, L.; Ammon, H. L. *J. Cryst. Mol. Struct.* **1974**, *4*, 63−75.
(49) Etter, M. C. *Acc. Chem. Res.* **1990**, *23*, 120−126.
(50) Graham, E. M.; Miskowski, V. M.; Perry, J. W.; Coulter, D. R.; Stiegman, A. E.; Schaefer, W. P.; Marsh, R. E. *J. Am. Chem. Soc.* **1989**, *111*, 8771−8779.
(51) Etter, M. C.; Frankenbach, G. M. *Chem. Mater.* **1989**, *1*, 10−12.
(52) Etter, M. C. *J. Phys. Chem.* **1991**, *95*, 4601−4610.
(53) Gebauer-Henke, E.; Tomkins, P.; Leitner, W.; Müller, T. E. *ChemCatChem* **2014**, *6*, 2910−2917.
(54) Kim, H. S.; Seo, S. H.; Lee, H.; Lee, S. D.; Kwon, Y. S.; Lee, I.-M. *J. Mol. Catal. A Chem.* **1998**, *132*, 267−276.
(55) Seidel-Morgenstern, A. *J. Chromatogr. A* **2004**, *1037*, 255−272.
(56) Woods, L. M.; Badescu, S. C.; Reinecke, T. L. *Phys. Rev. B* **2007**, *75*, 155415(1)−155415(9).